Electronic Supplementary Material (ESI) for ChemComm.

Asymmetrically Coordinated Zn-Co Diatomic Sites Catalyst for Efficient Hydrogen Evolution Reactions

*Jinhong Guo,[a‡] Jiayi Yang,[a‡] Zequn Xiang,[a‡] Huazhang Zhai, [*a] Wenxing Chen,[*a]*

Chemicals.

Zinc nitrate hexahydrate ($Zn(NO_3)_2 \cdot 6H_2O$), Cobaltous nitrate hexahydrate ($Co(NO_3)_2 \cdot 6H_2O$),Potassium bicarbonate ($KHCO_3$, 99.999%), Nafion D-521 dispersion (5% wt in water and 1-propanol), 2-methylimidazole, sulfur powder were purchased from Alfa Aesar. Dicyandiamide, methanol and ethanol were obtained from Sinopharm Chemical. All the chemicals and gases were analytical grade and used without further purification.

Synthesis.

Preparation of Zn_1Co_1-SNC DASC

The prepareration of the ZnCo-MOFs was referred to previous reported.[1] Typically, 2.94 g $Zn(NO_3)_2 \cdot 6H_2O$ and 120 mg $Co(NO_3)_2 \cdot 6H_2O$ were added synchronously into 80 ml of methanol solution for stirring 30 min. Then, 3.24 g 2-methylimidazole was dissolved in 80 ml methanol solution. The metal precursor solution was added immediately into the above ligand solution and stirred constantly for 5 h. The powders (ZnCo-MOFs) were obtained by washing with methanol for several times and drying at 60 °C in a vacuum oven for overnight. And the Zn_1Co_1-SNC DASC was obtained by the two-step pyrolysis strategy. Firstly, the sulfur powder (upstream) and ZnCo-MOFs powder (downstream) were placed successively in a tubular furnace, and then pyrolysis at 900 °C with a rate of 5 °C min^{-1}under an Ar atmosphere for 2 h. Secondly, the dicyandiamide (upstream) and the resulting sample (downstream) were then placed sequentially in a tubular furnace according to the above procedure, followed by a second pyrolysis at 1000 °C with a rate of 5 °C min^{-1} under Ar atmosphere for 2 h. The as-obtained Zn_1Co_1-SNC DASC catalyst was directly used for electrochemical and characterization tests without further treatment.

Preparation of Co_1-SNC Catalyst

The Co_1-SNC catalyst was prepared by similar procedures except for adding Co species and acid-etching process. In the synthetic procedure of Zn_1-SNC catalyst, the majority of low boiling point Zn atoms (mp 420 ℃, bp 907 ℃) could be evaporated away at high temperatures (1000 ℃), thus achieving the Co_1-SNC SAC.

Characterization.

Through a transmission electron microscope (TEM, JEOL JEM-2100F microscope, 200 kV) and a scanning electron microscope (SEM, JSM-6700F, 5 kV), the morphologies of samples were characterized. The X-ray powder diffraction (XRD) patterns of the samples were tested by X-ray powder diffraction (XRD, RigakuTTR-III X-ray diffractometer with Cu Kα radiation, λ =1.5418 Å). The atomic-resolution HAADF-STEM characterization was conducted using a probe aberration-corrected microscope, JEOL JEM-ARM200F equipped with cold emitter, an accelerating voltage of 200kV. X-ray photoelectron spectroscopy (XPS) was obtained by PerkinElmer Physics PHI 5300 energy spectrometer using mono-chromatic Al Kα radiation (1486.7 eV). At beamline BL12B of the National Synchrotron Radiation Laboratory (NSRL) of China, the X-ray absorption near-edge structure (XANES) spectra were tested.

XAFS measurements and analysis

The acquired EXAFS data were processed according to the standard procedures by using the ATHENA module of the IFEFFIT software packages. The detailed fitting process is stated below:

The obtained EXAFS spectra underwent the subtraction of post-edge background from the overall absorption and then normalization with respect to the edge-jump step. Subsequently, the χ(k) data were Fourier transformed to real (R) space by using a hanning windows (dk=1.0 Å^{-1}) to separate the EXAFS contributions from different coordination shells. To obtain the quantitative structural parameters around central atoms, least-squares curve parameter fitting was conducted by using the ARTEMIS module of the IFEFFIT software packages.

The following EXAFS equation was used:

$$\chi(k)=\sum_j \frac{N_j S_o^2 F_j(k)}{k R_j^2}\exp[-2k^2\sigma_j^2]\exp[\frac{-2R_j}{\lambda(k)}]\sin[2kR_j+\phi_j(k)]$$

In the equation, S_0^2 represent the amplitude reduction factor, $F_j(k)$ is the effective curved-wave backscattering amplitude, N_j is the number of neighbors in the j^{th} atomic shell, R_j represent the distance between the X-ray absorbing central atom and the atoms in the j^{th} atomic shell (backscatterer), λ represent the mean free path in Å, σ_j is the Debye-Waller parameter of the j^{th} atomic shell (variation of distances around the average R_j) and $\phi_j(k)$ is the phase shift (including the phase shift for each shell and the total central atom phase shift). The functions $F_j(k)$, λ and $\phi_j(k)$ were calculated with the ab initio code FEFF8.2

The coordination numbers of model samples (Co foil) were fixed as the nominal values. The obtained S_0^2 was fixed in the subsequent fitting of Zn_1Co_1-SNC sample. While the internal atomic distances *R*, Debye-Waller factor σ^2, and the edge-energy shift ΔE_0 were allowed to run freely.

Electrochemical Measurements.

The electrochemical measurements were carried out on a CHI 660e electrochemical workstation in a three-electrode configuration cell using as-prepared electrode as the working electrode, graphite rod as the counter electrode, and Ag/AgCl (saturated KCl) as the reference electrode in 0.5 M H_2SO_4 aqueous electrolyte. To prepare a homogeneous ink, 4 mg of the sample and 10 μL of a 5 wt% Nafion solution were dispersed in 1 mL of a water-isopropanol solution with a 1:1 volume ratio, followed by 30 min sonication. Then 20 μL of the dispersion (containing 80 μg of catalyst) wasloaded onto a glassy carbon electrode (5 mm in diameter, catalyst loading 0.408 mg cm^{-2}). The commercial 20 wt% Pt/C electrode was prepared using the same procedure for comparison. The LSV curves were conducted at scan rate of 20 mV/s. All of the potentials were quoted against a reversible hydrogen electrode (RHE).

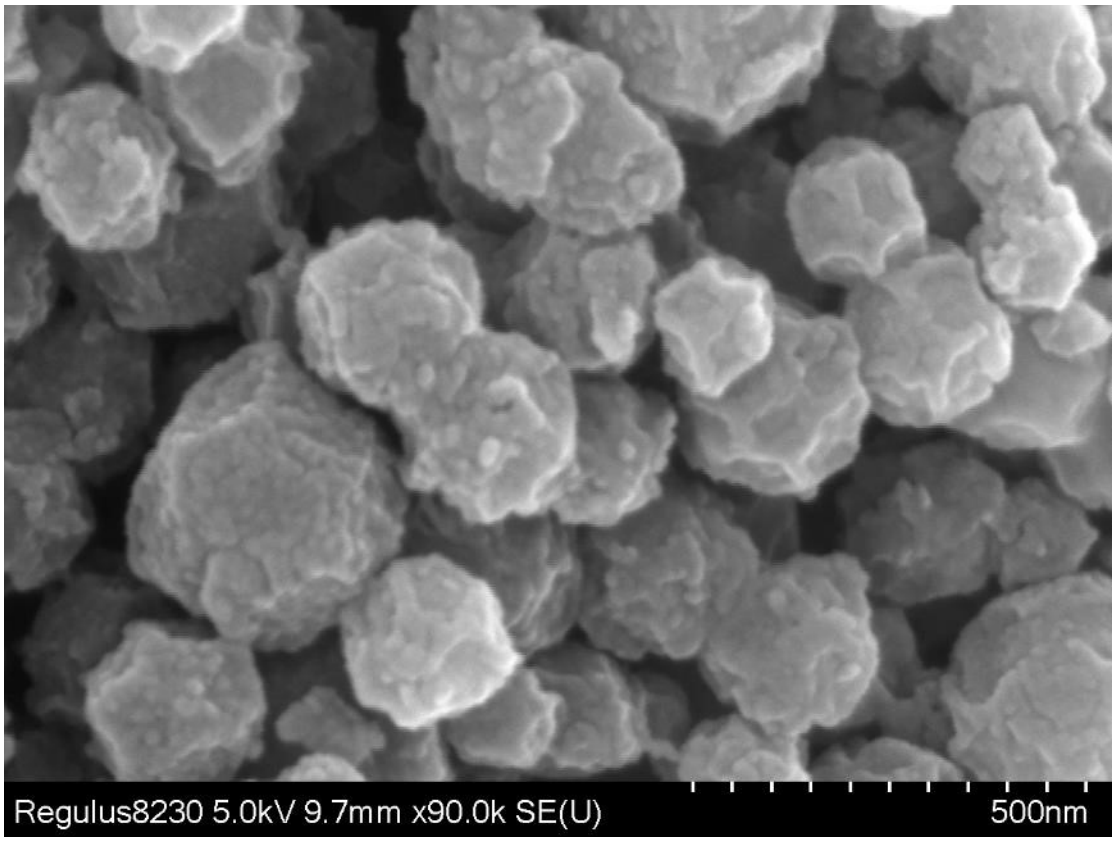

Figure S1. SEM image of Zn_1Co_1-SNC.

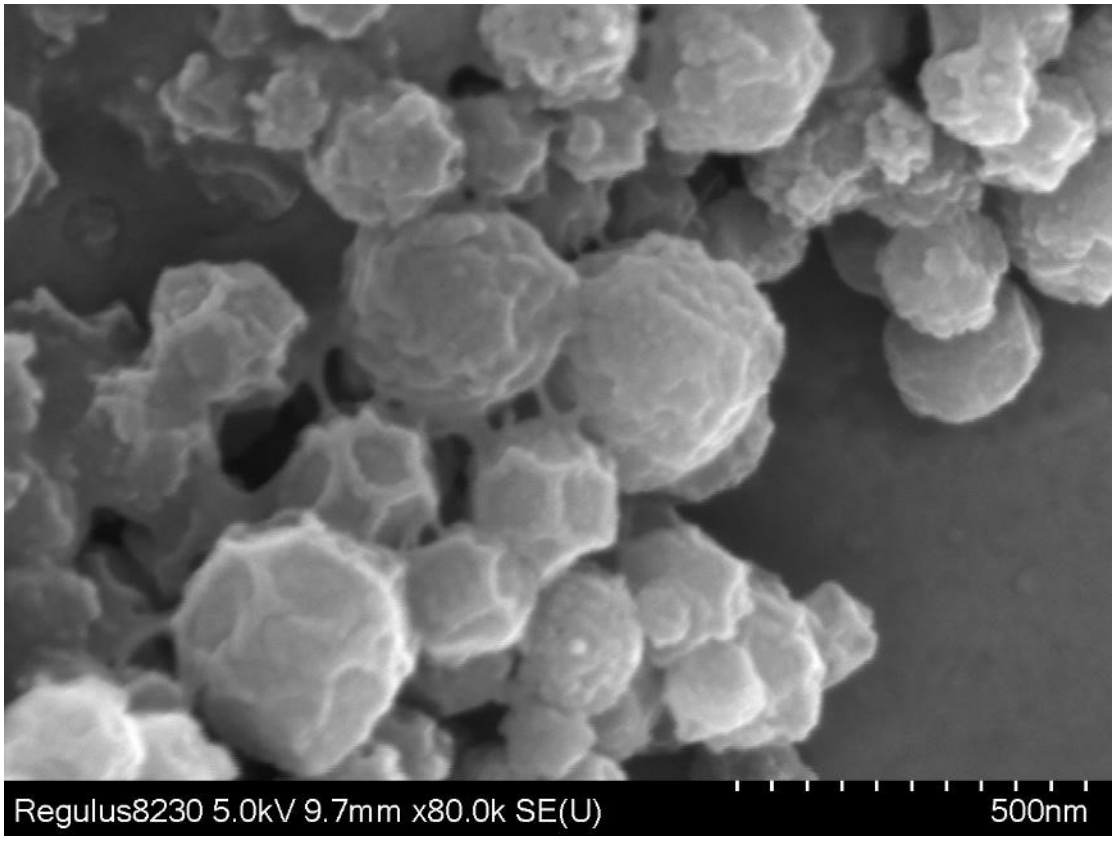

Figure S2. SEM image of Co_1-SNC.

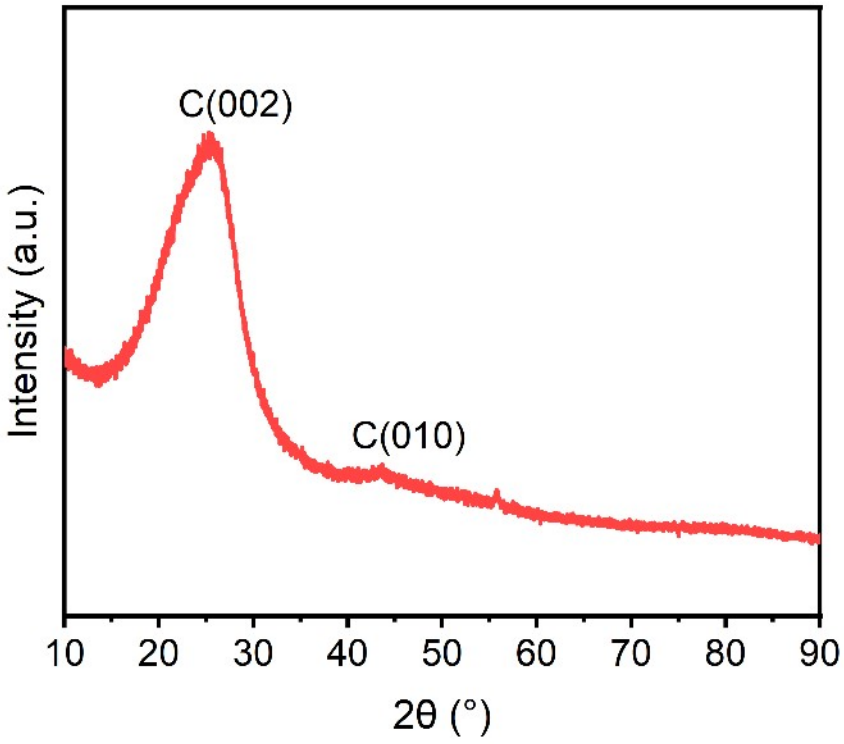

Figure S3. XRD pattern of Zn_1Co_1-SNC.

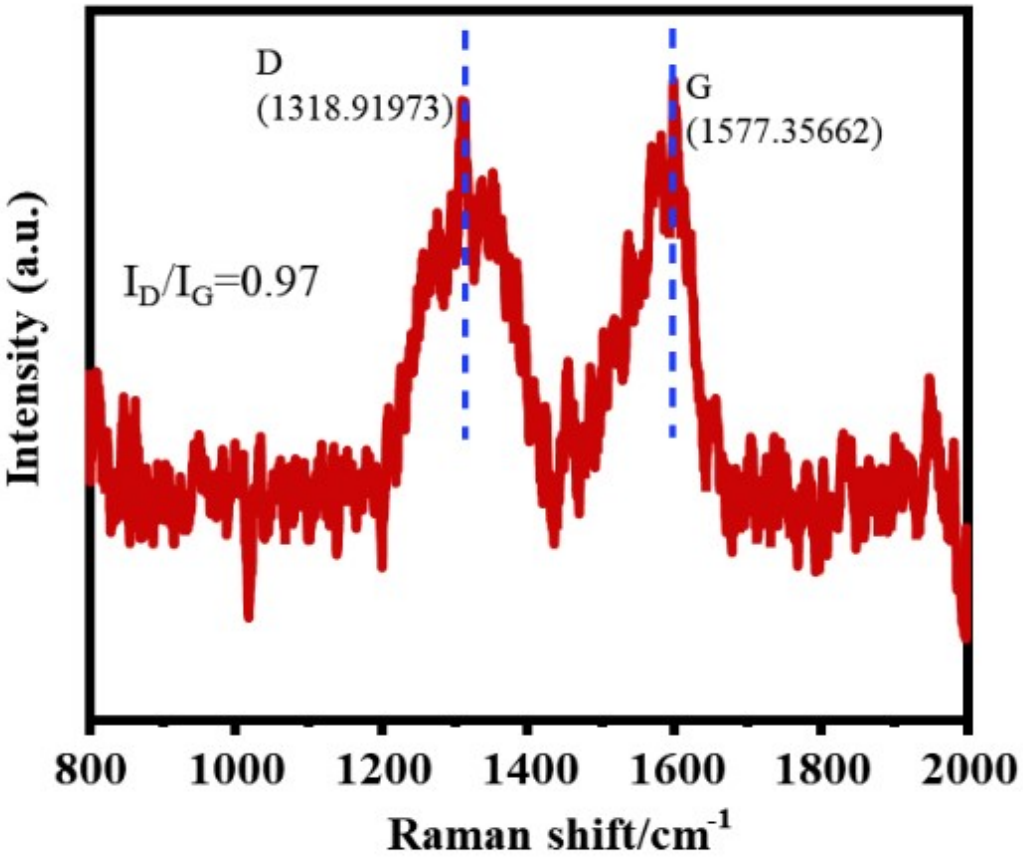

Figure S4. Raman pattern of Zn_1Co_1-SNC.

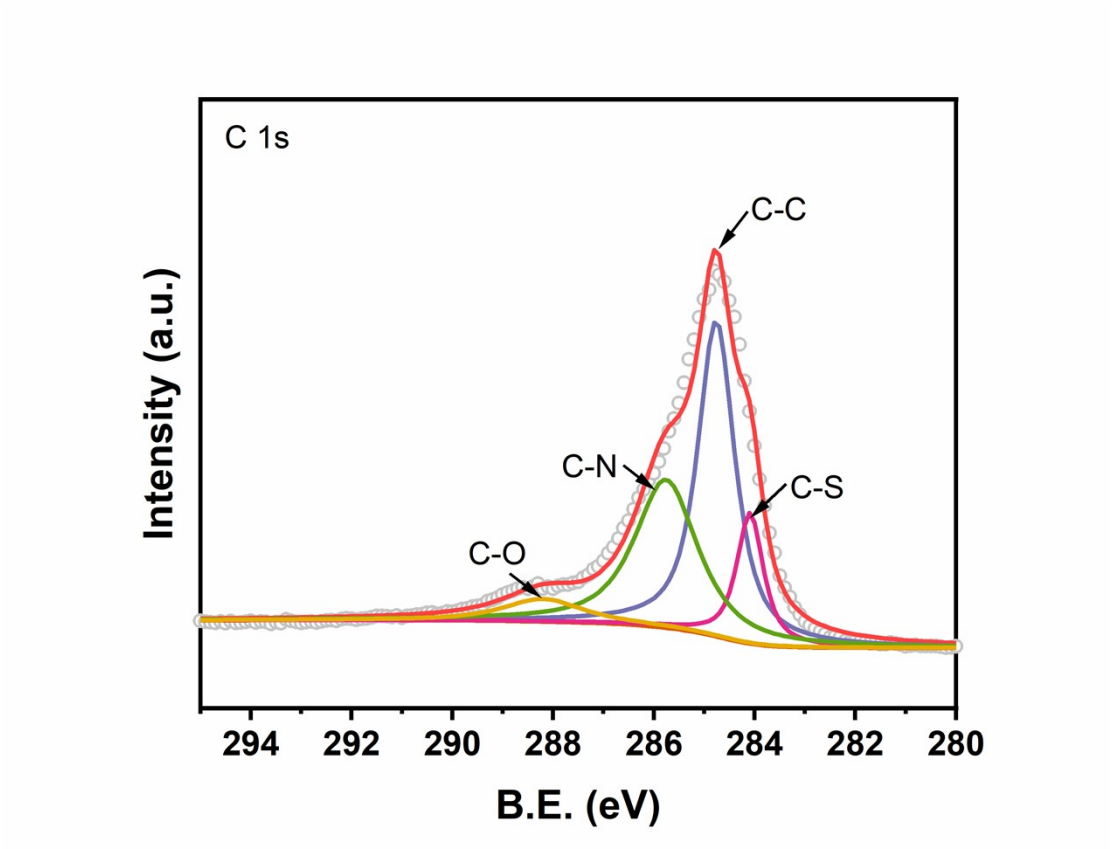

Figure S5. High-resolution C 1s XPS spectra of Zn_1Co_1-SNC DASC.

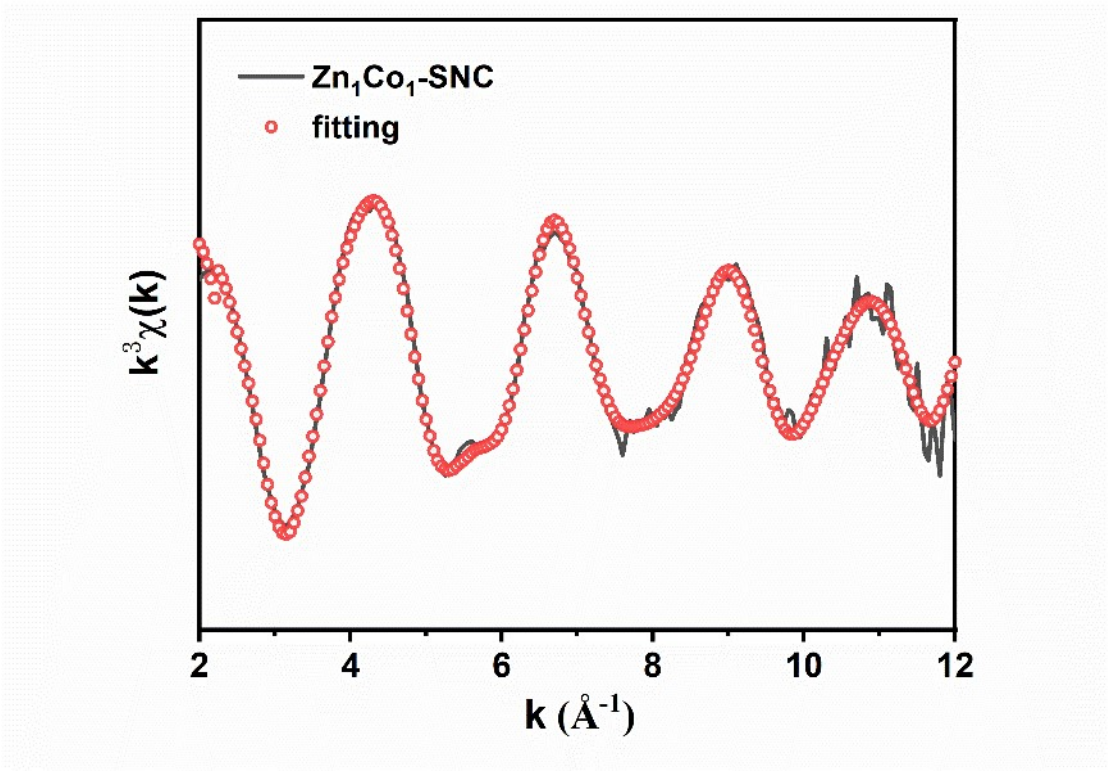

Figure S6. The EXAFS fitting results of Zn_1Co_1-SNC at Co K-edge.

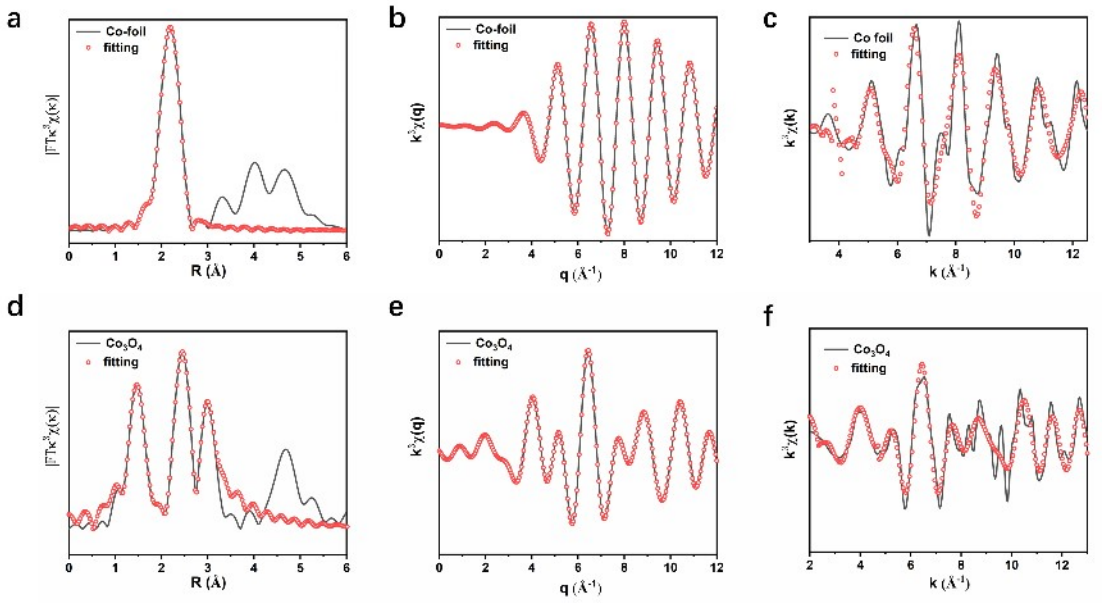

Figure S7. The EXAFS fitting results of Co foil at Co K-edge. (a) R space, (b) q space and (c) k space. The EXAFS fitting results of Co_3O_4 at Co K-edge. (d) R space, (e) q space and (f) k space.

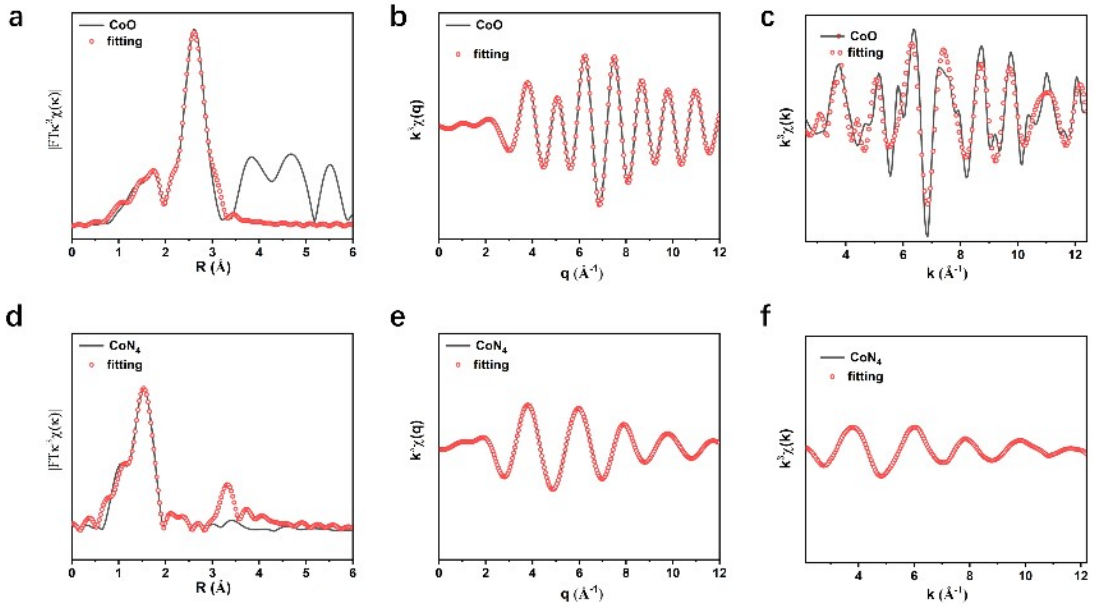

Figure S8. The EXAFS fitting results of CoO at Co K-edge. (a) R space, (b) q space and (c) k space. The EXAFS fitting results of CoN_4 at Co K-edge. (d) R space, (e) q space and (f) k space.

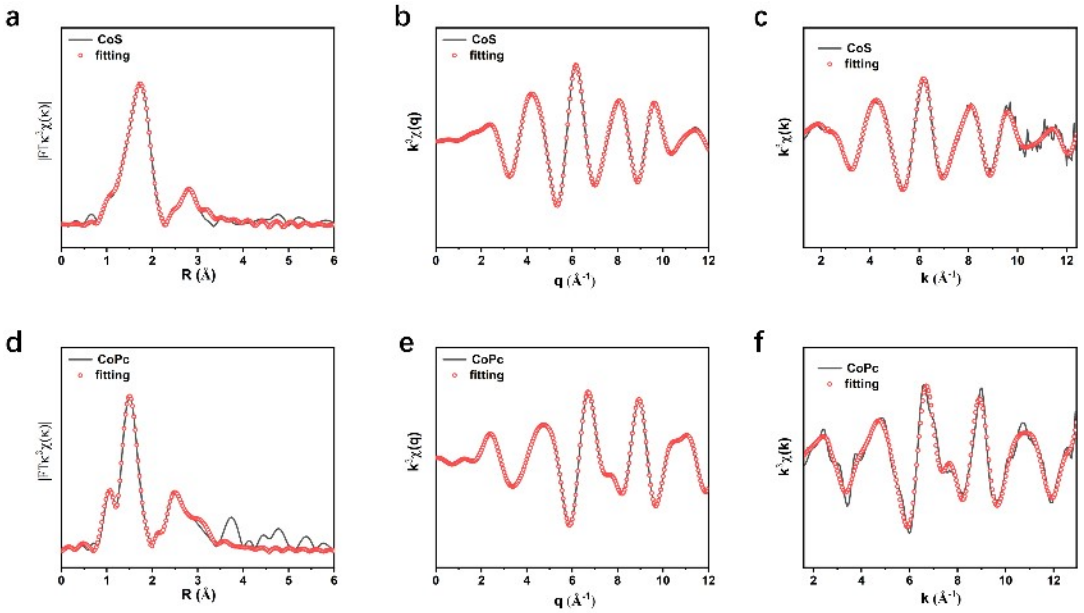

Figure S9. The EXAFS fitting results of CoS at Co K-edge. (a) R space, (b) q space and (c) k space. The EXAFS fitting results of CoPc at Co K-edge. (d) R space, (e) q space and (f) k space.

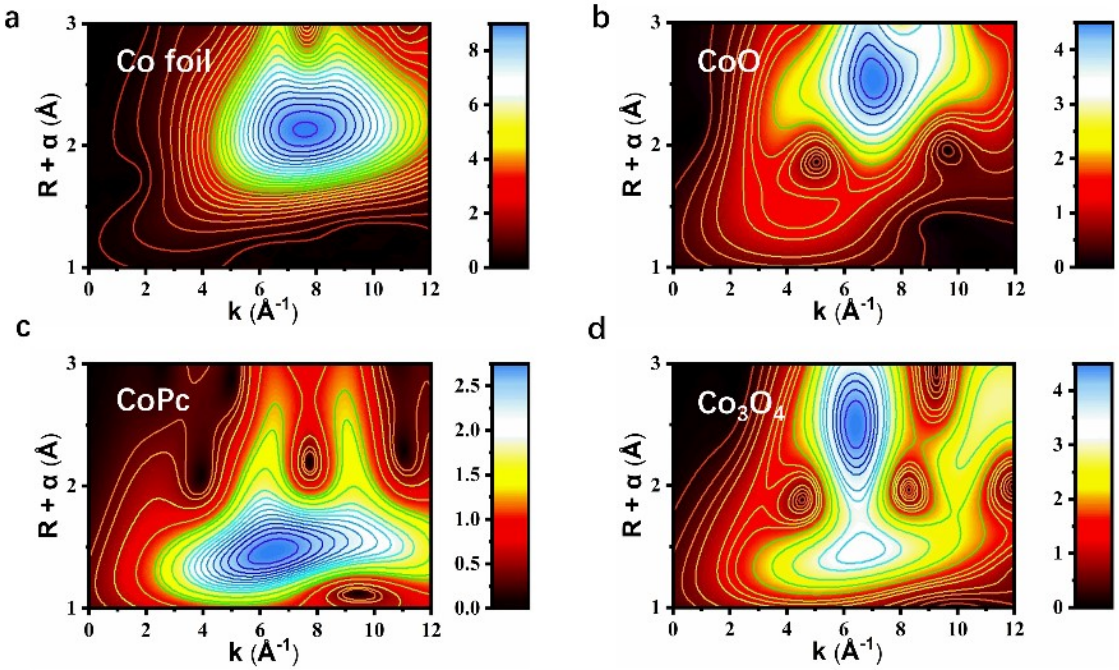

Figure S10. WT-EXAFS plots of (a) Co foil, (b) CoO, (c) CoPc and (d) Co_3O_4.

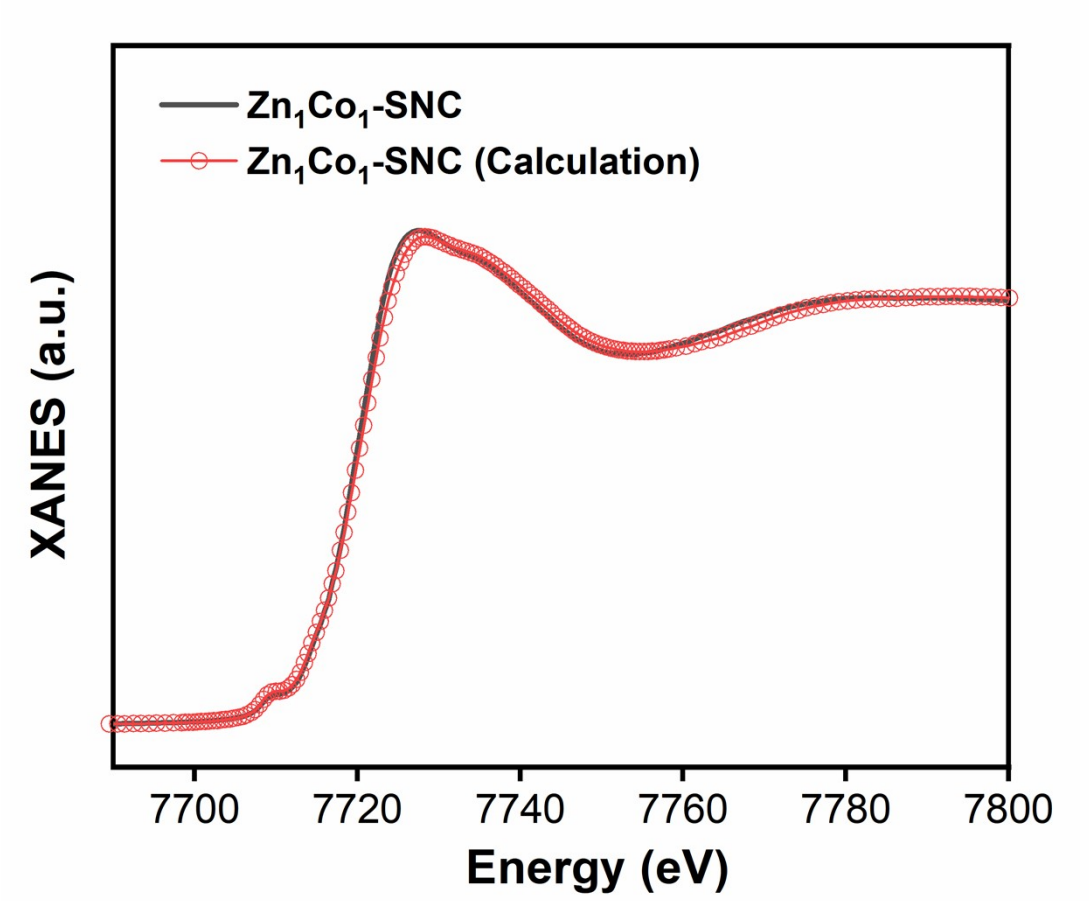

Figure S11. Experimental XANES and calculated XANES curves of Zn_1Co_1-SNC at Co K-edge.

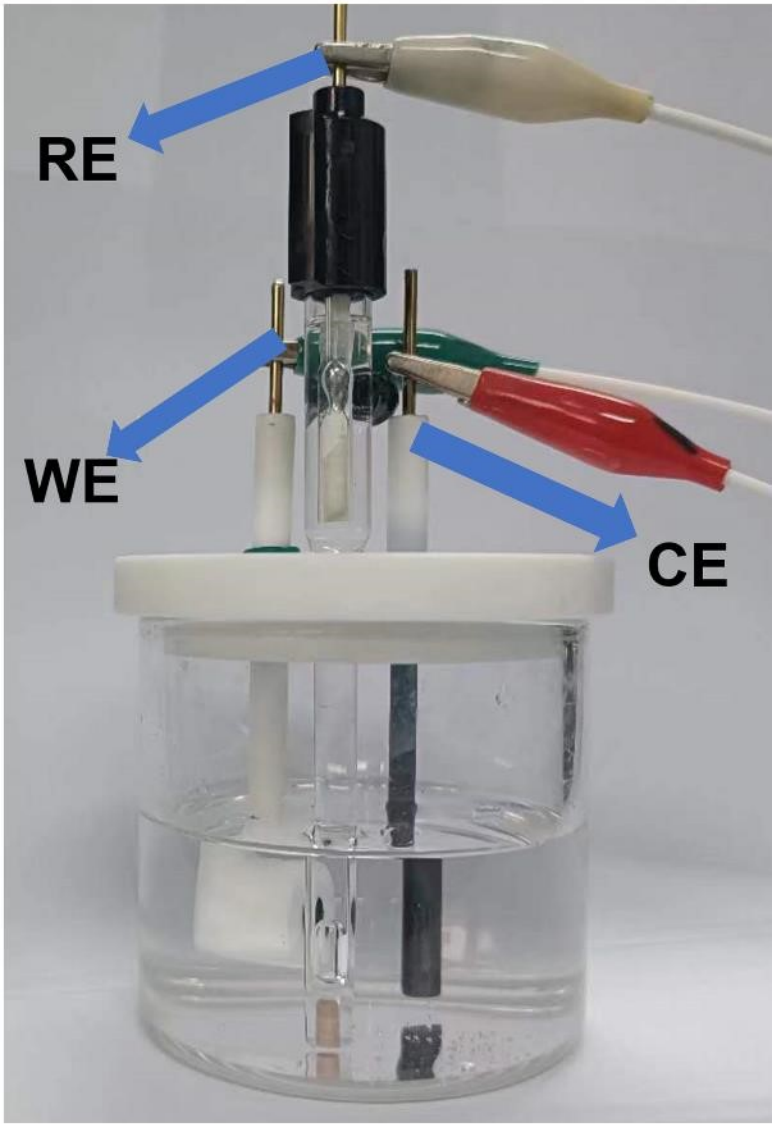

Figure S12. Photograph of the typical three-electrode setup for the electrochemical HER measurements. (The red electrode clamp is connected to the counter electrode, the white electrode clamp is connected to the reference electrode, and the green electrode clamp is connected to the working electrode)

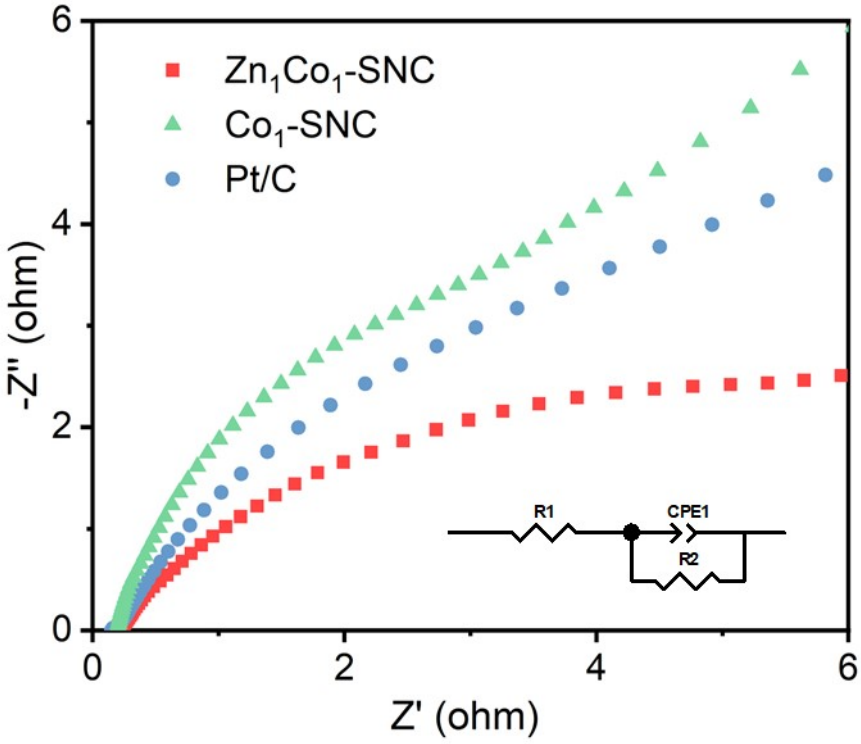

Figure S13. Nyquist plots of the Zn_1Co_1-SNC, Co_1-SNC, and Pt/C at the overpotential of 50 mV.

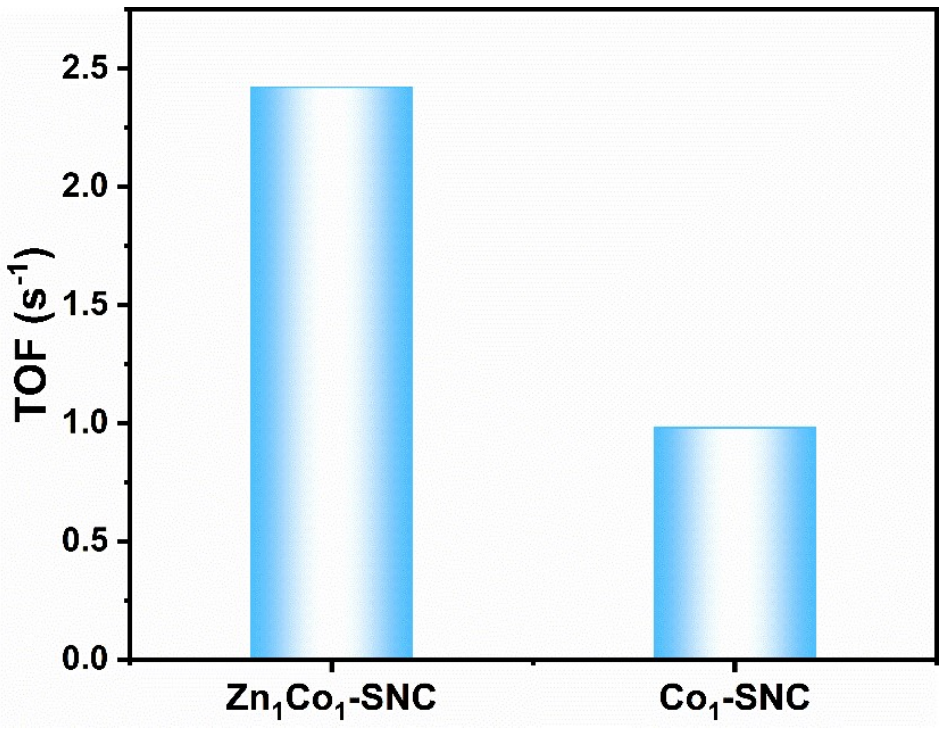

Figure S14. TOF value of Zn_1Co_1-SNC and Co_1-SNC (η = 100 mV)

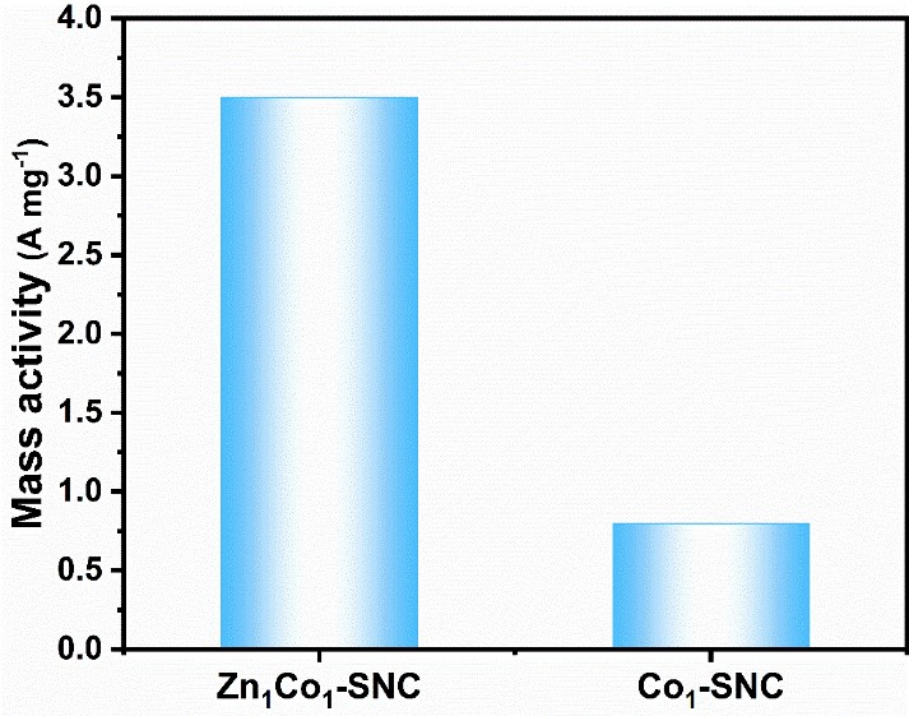

Figure S15. Mass activity (40mV) of Zn_1Co_1-SNC, and Co_1-SNC.

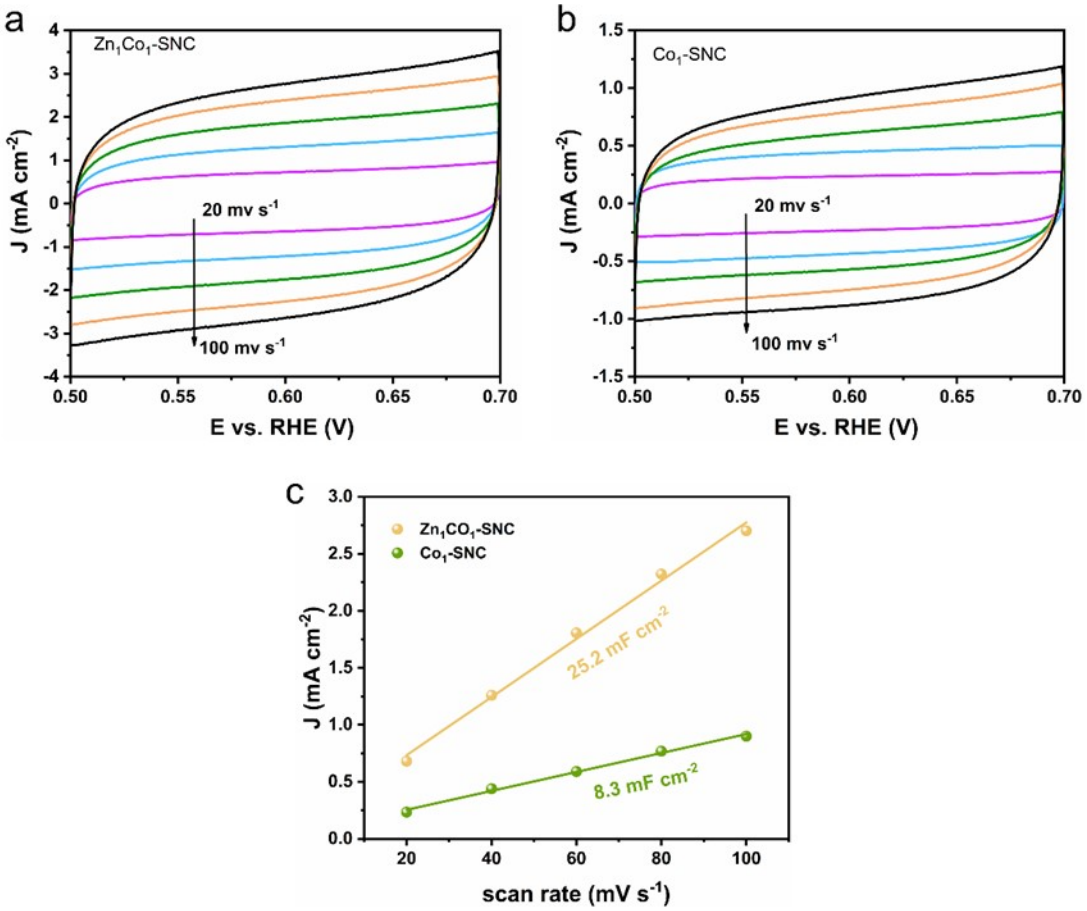

Figure S16. CV curves of obtained samples and corresponding C_{dl} and ECSA in 0.5 M H_2SO_4

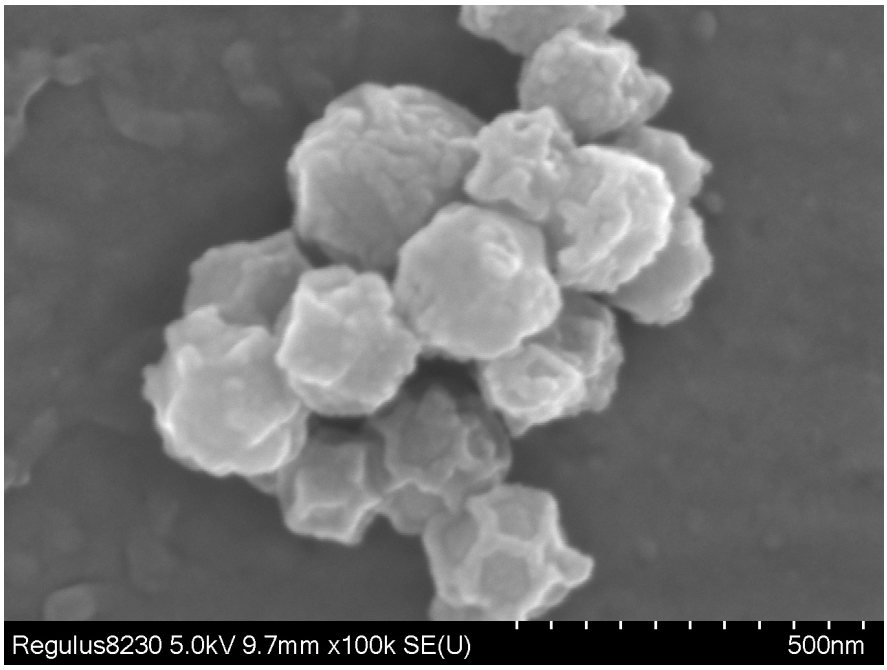

Figure S17. SEM image of Zn_1Co_1-SNC after durability test.

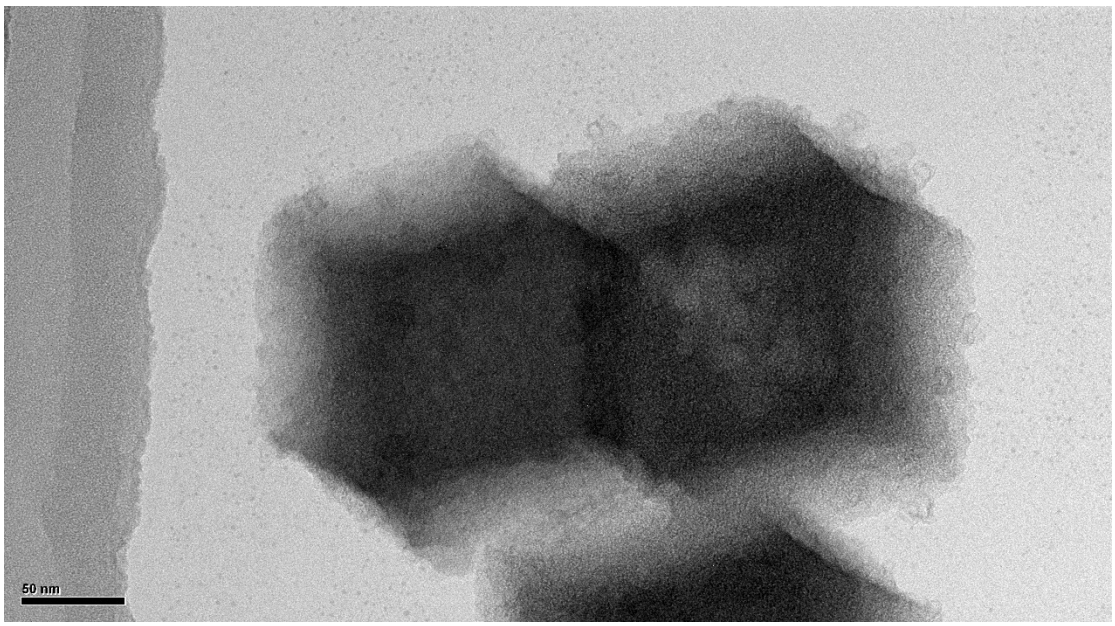

Figure S18. TEM image of Zn_1Co_1-SNC after durability test.

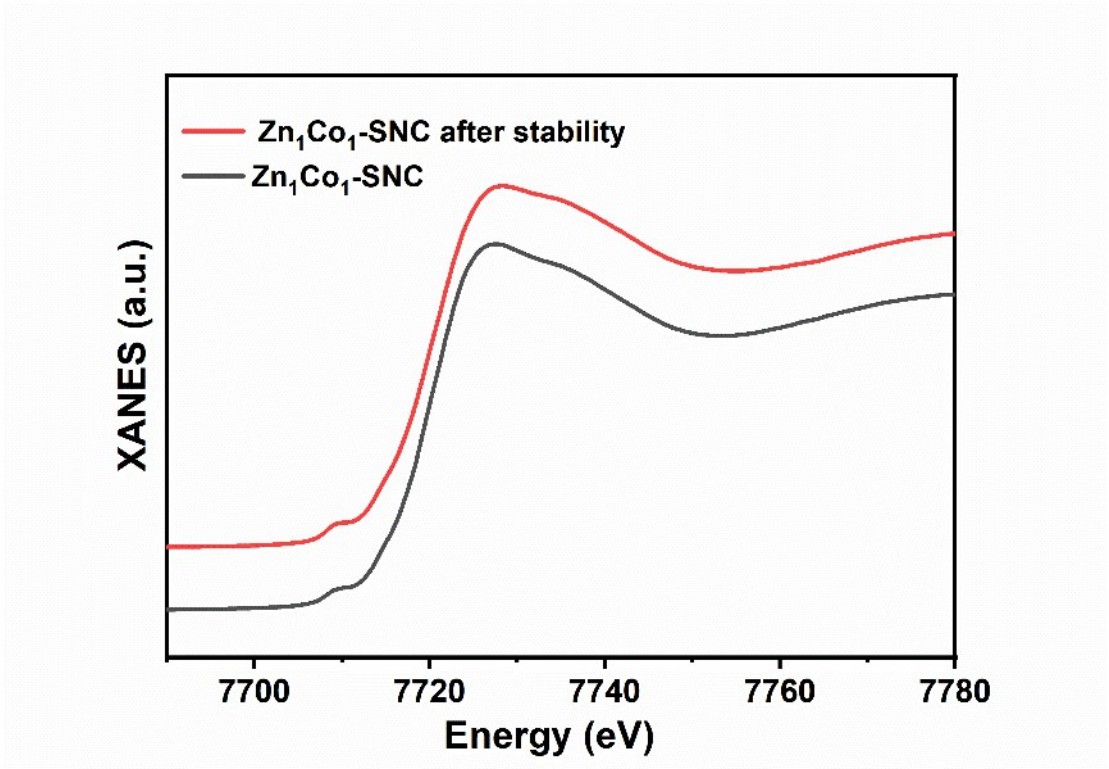

Figure S19. XANES of Zn_1Co_1-SNC after durability test.

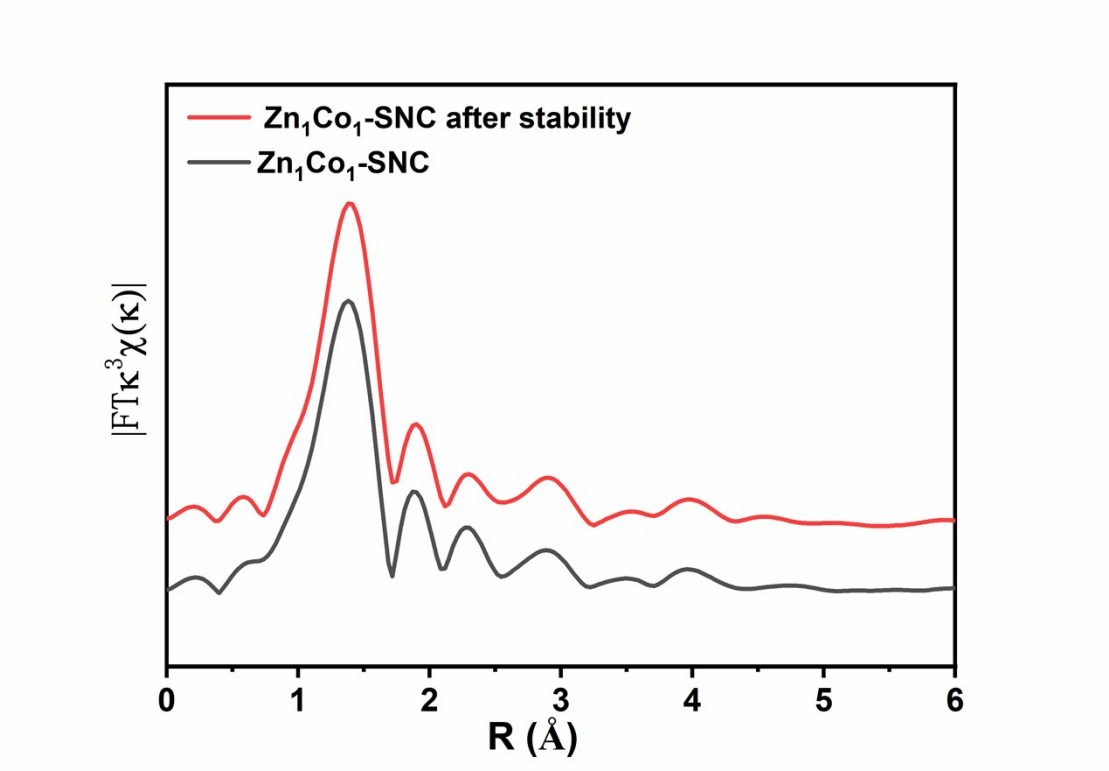

Figure S20. EXAFS of Zn_1Co_1-SNC after durability test.

Table S1. Structural parameters extracted from Co K-edge EXAFS fitting. (S_0^2=0.84).

Sample	Path	CN	R(Å)	σ^2(10^{-3}Å^2)	ΔE_0(eV)	R factor
Zn_1Co_1-SNC	Co-N	1.9±0.4	1.96±0.02	5.7	2.1	0.012
	Co-S	1.0±0.3	2.33±0.02	9.3		
	Co-Zn	1.1±0.2	2.50±0.02	7.8		
CoN_4	Co-N	3.9±0.6	1.90±0.02	2.1	1.4	0.008
Co foil	Co-Co	12.0*	2.49±0.01	7.9	5.8	0.002

S_0^2 is the amplitude reduction factor; CN is the coordination number; R is interatomic distance (the bond length between Co central atoms and surrounding coordination atoms); σ^2 is Debye-Waller factor (a measure of thermal and static disorder in absorber-scatterer distances); ΔE_0 is edge-energy shift (the difference between the zero kinetic energy value of the sample and that of the theoretical model). R factor is used to value the goodness of the fitting.

Table S2. Summary of various Co based catalysts in acidic condition at 10 mA cm^{-2}.

Material	Electrolyte	Overpotential /mV	Tafel slope/(mV dec^{-1})	Ref.
Zn_1Co_1-SNC	0.5 M H_2SO_4	49	48	This Work
Zn/SNC	0.5 M H_2SO_4	124	78	This Work
Co-P@PC	0.5 M H_2SO_4	72	49	1
Co−I−N/G	0.5 M H_2SO_4	52	56	2
Co-3C1N	0.5 M H_2SO_4	138	55	3
Co/Co_xS_y@NC	0.5 M H_2SO_4	130	82	4
Co-MoS_2/G	0.5 M H_2SO_4	78.1	40	5
Co-N_4C_4	0.5 M H_2SO_4	175	80	6
Co-NG	0.5 M H_2SO_4	147	82	7
Co_3O_4–Mo_2N	0.5 M H_2SO_4	60	162.4	8

References

1. J. Wu, D. Wang, S. Wan, H. Liu, C. Wang and X. Wang, *Small*, 2019, **16**.
2. J. Liu, D. Wang, K. Huang, J. Dong, J. Liao, S. Dai, X. Tang, M. Yan, H. Gong, J. Liu, Z. Gong, R. Liu, C. Cui, G. Ye, X. Zou and H. Fei, *ACS Nano*, 2021, **15**, 18125-18134.
3. Z.-L. Wang, X.-F. Hao, Z. Jiang, X.-P. Sun, D. Xu, J. Wang, H.-X. Zhong, F.-L. Meng and X.-B. Zhang, *J. Am. Chem. Soc.*, 2015, **137**, 15070-15073.
4. H. D. Mai, P. M. Park, G.-N. Bae, S. Jeong, B. Seo, M. Cho, S. Park, N. D. Cuong, T. V. Cuong, N. M. Tran, C.-M. Park and K.-J. Jeon, *J. Mater. Chem. A*, 2024, **12**, 4761-4769.
5. S. Sarwar, M.-C. Lin, M. R. Ahasan, Y. Wang, R. Wang and X. Zhang, *Adv. Compos. Hybrid Mater.*, 2022, **5**, 2339-2352.
6. H. Fei, J. Dong, C. Wan, Z. Zhao, X. Xu, Z. Lin, Y. Wang, H. Liu, K. Zang, J. Luo, S. Zhao, W. Hu, W. Yan, I. Shakir, Y. Huang and X. Duan, *Adv. Mater.*, 2018, **30**.
7. H. Fei, J. Dong, M. J. Arellano-Jiménez, G. Ye, N. Dong Kim, E. L. G. Samuel, Z. Peng, Z. Zhu, F. Qin, J. Bao, M. J. Yacaman, P. M. Ajayan, D. Chen and J. M. Tour, *Nat. Commun.*, 2015, **6**.
8. T. Wang, P. Wang, W. Zang, X. Li, D. Chen, Z. Kou, S. Mu and J. Wang, *Adv. Funct. Mater.*, 2021, **32**.